Magnetic second-harmonic generation of an antiferromagnetic film

Siew-Choo Lim

School of Physics, Universiti Sains Malaysia, 11800 Minden, Penang, Malaysia

Received August 9, 2001; revised manuscript received November 2001

Second-harmonic generation of an antiferromagnetic film in Voigt geometry is calculated and analyzed. This calculation is carried out with an assumption of weak nonlinearity in a two-sublattice antiferromagnetic system. Second-harmonic waves are analyzed by the conventional approach of ordinary nonlinear optics.

OCIS code: 190.0190

1. INTRODUCTION

The simplest nonlinear response in a physical system that has been subjected to incident electromagnetic radiation is second-harmonic generation (SHG) in the weak nonlinear regime.[1] This weak nonlinear approach is usually used in the study of nonlinear effects in dielectrics,[1,2] and it has been extended to magnetic systems.[3–7] This approach offers a simpler way to study various nonlinear effects, especially SHG and optical rectification in magnetic systems and intensity-dependent third-order effects such as multistability and soliton propagation in magnetic films.[5,6]

A previous calculation revealed that among various types of magnetic system the simplest two-sublattice antiferromagnet is a weak nonlinear system.[4] The antiferromagnets that are well described by the two-sublattice model are FeF_2 and MnF_2.[8] With the weak nonlinearity in these antiferromagnetic systems we can use the conventional methods of nonlinear optics to analyze antiferromagnetic nonlinear responses. With this assumption, the sublattice magnetization is expanded in power series of the incident dynamic magnetic fields, h:

$$m_i = \chi_{ij}h_j + \chi_{ijk}h_jh_k + \chi_{ijkl}h_jh_kh_l + \dots . \quad (1)$$

Based on Eq. (1) and the Landau–Lifshitz torque equations of motion for magnetization,[9] the complete linear and nonlinear susceptibility tensors up to third-order effects for a single-frequency incident field were calculated and analyzed.[4] Parts of the nonvanishing tensor elements and their applications have been calculated and analyzed by Almeida and Mills[5] and by Vukovich *et al.*[6] These are intensity-dependent third-order tensor elements that cause bistable and multistable transmission through antiferromagnetic films in the presence of applied static magnetic fields.

In this paper the most fundamental nonlinear effect, SHG through an antiferromagnetic film, is calculated and analyzed based on second-harmonic tensor elements calculated previously.[4] In Section 2 a way to determine the appropriate geometry from the nonvanishing tensor elements for observation of second harmonic (SH) waves generated through an antiferromagnetic film is described. In Section 3 the propagation of linear and SH waves in an antiferromagnetic medium (AFM) is described for two cases: phase mismatching and phase matching. The solutions for transmission T and reflection R of linear waves and for transmission $\mathcal{T}$ and reflection $\mathcal{R}$ of SH waves through the film are given in Section 4. In Section 5, the results of the calculations in Sections 3 and 4, together with their implications, are shown graphically by use of FeF_2 parameters. Finally, a brief conclusion is given in Section 6.

2. MODELING

To determine a suitable model for the observation of SH effects, we review here the nonvanishing susceptibility tensor elements. Previous calculations have determined the independent nonvanishing linear and nonlinear elements up to SH effects in a circular polarization system (pnz): χ_{pp}, χ_{nn}, χ_{ppz}, χ_{nnz}, and χ_{zpn}. The complete mathematical expressions of these elements are given in Appendix A. These tensor elements can be transformed into a Cartesian system (xyz) by use of the following definitions:

$$S_k = U_{k\delta}S_\delta \quad (2)$$

with the inverse

$$S_\theta = T_{\theta l}S_l , \quad (3)$$

where

$$U_{k\delta} = \begin{bmatrix} \frac{1}{\sqrt{2}} & \frac{1}{\sqrt{2}} & 0 \\ -\frac{i}{\sqrt{2}} & \frac{i}{\sqrt{2}} & 0 \\ 0 & 0 & 1 \end{bmatrix}, \quad (4)$$

0740-3224/2002/060001-10$15.00

$$T_{\theta l} = \begin{bmatrix} \frac{1}{\sqrt{2}} & \frac{i}{\sqrt{2}} & 0 \\ \frac{1}{\sqrt{2}} & -\frac{i}{\sqrt{2}} & 0 \\ 0 & 0 & 1 \end{bmatrix}. \tag{5}$$

Here the subscripts l and k refer to (xyz) and the subscripts θ and δ refer to (pnz). For calculation of SHG it is convenient to transform the tensor components from the (pnz) to the (xyz) framework:

$$\chi_{ij} = T_{i\alpha}T_{j\beta}\chi_{\alpha\beta}, \tag{6}$$

$$\chi_{ijk} = T_{i\alpha}T_{j\beta}T_{k\gamma}\chi_{\alpha\beta\gamma}, \tag{7}$$

where subscripts in roman type refer to (xyz) and those in greek to (pnz), and T is the complex rotation matrix defined in Eq. (5). The nonvanishing linear and SHG components in the (xyz) framework are

$$\chi_{xx} = \chi_{yy} = {}^1/_2(\chi_{pp} + \chi_{nn}), \tag{8}$$

$$\chi_{xy} = -\chi_{yx} = {}^{1/2}/_i(\chi_{pp} - \chi_{nn}), \tag{9}$$

$$\chi_{xxz} = \chi_{yyz} = {}^1/_2(\chi_{ppz} + \chi_{nnz}), \tag{10}$$

$$\chi_{xyz} = -\chi_{yxz} = (i/2)(\chi_{ppz} - \chi_{nnz}), \tag{11}$$

$$\chi_{zxx} = \chi_{zyy} = {}^1/_2\chi_{znp}. \tag{12}$$

From these nonvanishing elements we can determine the configuration of the antiferromagnetic samples for the generation of SH waves effectively. The simplest method for doing so is to cause a rf field to be incident normally upon a film and to analyze the transmission and reflection through the film. For this purpose there are two possible configurations for magnetic systems: Faraday geometry and Voigt geometry. For Faraday geometry the configuration of the film and of the incident rf field is as shown in Fig. 1.

For plane waves incident in the $-z$ direction and with polarization in the x–y plane we can observe linear transmission T and reflection R for low intensity of I. For a sufficiently intense rf field in I we can observe bistable and multistable transmission through the film with the same frequency as I and third-harmonic waves caused by nonvanishing third-harmonic-generation tensor elements.[4,5] However, no transverse SH waves can be seen to be transmitted and reflected through the film. Because for the x- and y-polarized waves in the incident rf fields the nonvanishing SH tensor elements are χ_{zxx} and χ_{zyy} only, the transverse SH waves that are generated will be z polarized and will propagate in the x–y plane.

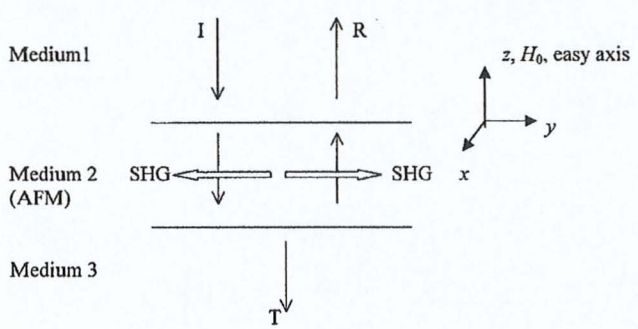

Fig. 1. Antiferromagnetic film in Faraday geometry.

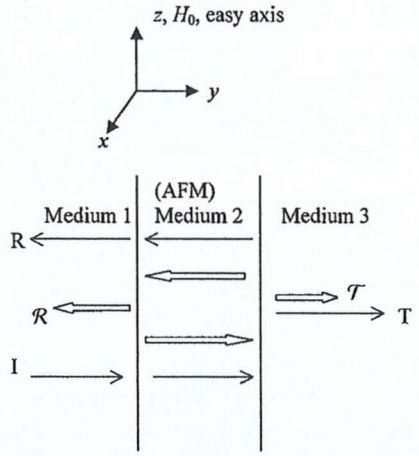

Fig. 2. Antiferromagnetic film in Voigt geometry.

For Voigt geometry the configuration of the film and of the incident rf field is as given in Fig. 2. For plane waves incident in the y direction and with x polarization only, the tensor elements that correspond to SHG are the same as in the Faraday geometry: χ_{zxx} and χ_{zyy}. We can observe linear transmission T and reflection R for low intensity of I. For a sufficiently intense rf field in I, transmission $\mathcal{T}$ and reflection $\mathcal{R}$ of z-polarized SH waves through the film can be observed as well. Therefore the transmission and reflection of SH waves through an antiferromagnetic film can best be seen in an antiferromagnetic film in the Voigt geometry configuration, as in Fig. 2. Based on this conclusion, detailed calculations and analyses of SHG effects through an antiferromagnetic film are given in the following sections.

3. PROPAGATION OF LINEAR AND SECOND-HARMONIC WAVES IN VOIGT GEOMETRY

In the previous calculations[4] all the linear and nonlinear susceptibility tensor elements up to third-order effects for a two-sublattice AFM system were derived based on interactions with polarizations and frequencies of the incident radiation. In actual applications and calculations of nonlinear effects such as SHG and bistability, not all the elements correspond to these effects. The way in which the model is constructed, such as by Voigt configurations, and the direction of incident radiation will determine which elements should be taken into account as a result of the transverse nature of electromagnetic waves.

In Voigt geometry, for an x-polarized incident rf magnetic field the wave equations derived from Maxwell's equations and the appropriate constitutive relations are

$$\frac{\partial^2 H_{x0}(y)}{\partial y^2} + k_V{}^2 H_{x0}(y) = 0 \tag{13}$$

for linear waves and

$$\frac{\partial^2 H_{z0}(y)}{\partial y^2} + k_z{}^2 H_{z0}(y) = \Gamma H_{x0}(y) H_{x0}(y) \tag{14}$$

for SH waves. Here k_V and k_z represent the magnitudes of linear and SH propagation vectors, respectively, and Γ is a function of linear and SH susceptibility elements and corresponds to the generation of SH waves. The mathematical derivations are outlined in Appendix B. Equation (13) is a homogeneous linear second-order differential equation for $H_{x0}(y)$, and Eq. (14) is an inhomogeneous linear second-order differential equation for $H_{z0}(y)$ with a source in terms of $H_{x0}(y)$. The results in Eqs. (13) and (14) were obtained by a weak nonlinearity approach and without the slowly varying envelope approximation. In the calculation it was assumed that there is no depletion of the input waves. Based on Eq. (13) the general solutions for the linear waves, $H_x(y, t)$ and $E_z(y, t)$, are

$$H_x(y, t) = \tfrac{1}{2}[a \exp(ik_V y) + b \exp(-ik_V y)] \times \exp(-i\omega t) + \text{c.c.}, \quad (15)$$

$$E_z(y, t) = \frac{1}{2}\frac{k_V}{\epsilon_0 \epsilon \omega}[a \exp(ik_V y) - b \exp(-ik_V y)] \times \exp(-i\omega t) + \text{c.c.} \quad (16)$$

From Eq. (14), the general solutions for SH waves $H_z(y, t)$ and $E_x(y, t)$ are

$$H_z(y, t) = \tfrac{1}{2}[\alpha \exp(ik_z y) + \beta \exp(-ik_z y) + f_1 \exp(i\xi y) + f_2 \exp(-i\xi y) + f_3]\exp(-i\Omega t) + \text{c.c.}, \quad (17)$$

$$E_x(y, t) = \frac{1}{2}\frac{1}{\epsilon_0 \epsilon \Omega}[-\alpha k_z \exp(ik_z y) + \beta k_z \exp(-ik_z y) - f_1 \xi \exp(i\xi y) + f_2 \xi \exp(-i\xi y)] \times \exp(-i\Omega t) + \text{c.c.}, \quad (18)$$

where

$$f_1 = \frac{\Gamma a^2}{(k_z{}^2 - \xi^2)}, \qquad f_2 = \frac{\Gamma b^2}{(k_z{}^2 - \xi^2)}, \qquad f_3 = \frac{2ab\Gamma}{k_z{}^2} \quad (19)$$

for phase mismatch ($k_z \neq 2k_V = \xi$) and

$$H_z(y, t) = \tfrac{1}{2}[(\alpha + yd_1)\exp(i\xi y) + (\beta + yd_2) \times \exp(-i\xi y) + d_3]\exp(-i\Omega t) + \text{c.c.}, \quad (20)$$

$$E_x(y, t) = \frac{1}{2}\frac{1}{\epsilon_0 \epsilon \Omega}[(-\alpha\xi + id_1 - \xi y d_1)\exp(i\xi y) + (\beta\xi + id_2 + \xi y d_2) \times \exp(-i\xi y)]\exp(-i\Omega t) + \text{c.c.}, \quad (21)$$

where

$$d_1 = \frac{\Gamma a^2}{i2\xi}, \qquad d_2 = \frac{\Gamma b^2}{-i2\xi}, \qquad d_3 = \frac{2ab\Gamma}{\xi^2} \quad (22)$$

for phase matching ($k_z = 2k_V = \xi$). The terms a, b and α, β are the superposition coefficients for the homogeneous solutions of Eqs. (13) and (14), respectively, and are determined by the appropriate boundary conditions. The mathematical details of Eqs. (13)–(22) and definitions of the terms are given in Appendix B.

4. TRANSMISSION AND REFLECTION OF LINEAR AND SECOND-HARMONIC WAVES

Applying the antiferromagnetic film boundary conditions to the tangential H and E fields in Section 3 as shown in the schematic diagram of Fig. 2, i.e., the continuity of these rf fields across the film boundaries, yields the coefficients for the transmitted and reflected amplitudes:

$$t = \theta^{-1}(a\delta + b\delta^{-1}), \quad (23)$$

$$r = a + b - p, \quad (24)$$

where

$$a = \frac{2q_1(q_V + q_3)p}{(q_1 + q_V)(q_V + q_3) + (q_1 - q_V)(q_V - q_3)\delta^2}, \quad (25)$$

$$b = \frac{2q_1(q_V - q_3)\delta^2 p}{(q_1 + q_V)(q_V + q_3) + (q_1 - q_V)(q_V - q_3)\delta^2} \quad (26)$$

for linear waves. Details of the derivations and definitions of the terms in this section are given in Appendix C.

For SH waves the coefficients for the transmitted and the reflected amplitudes are, respectively,

$$\tau = (\alpha\Delta + \beta\Delta^{-1} + \phi_{\text{hr}})\Pi^{-1}, \quad (27)$$

$$\rho = \alpha + \beta + \phi_{\text{hl}}, \quad (28)$$

where

$$\alpha = \frac{(\eta_z + \eta_3)(\phi_{\text{el}} - \eta_1\phi_{\text{hl}})\Delta^{-1} + (\eta_1 - \eta_z)(\phi_{\text{er}} + \eta_3\phi_{\text{hr}})}{(\eta_1 + \eta_z)(\eta_z + \eta_3)\Delta^{-1} - (\eta_1 - \eta_z)(\eta_3 - \eta_z)\Delta}, \quad (29)$$

$$\beta = \frac{-(\eta_1 + \eta_z)(\phi_{\text{er}} + \eta_3\phi_{\text{hr}}) - (\eta_3 - \eta_z)(\phi_{\text{el}} - \eta_1\phi_{\text{hl}})\Delta}{(\eta_1 + \eta_z)(\eta_z + \eta_3)\Delta^{-1} - (\eta_1 - \eta_z)(\eta_3 - \eta_3)\Delta}. \quad (30)$$

In this case, $\phi_{ij} = U_{ij}$ for phase mismatching and $\phi_{ij} = V_{ij}$ for phase matching. The explicit expressions for U_{ij} and V_{ij} and the derivations for Eqs. (27)–(30) are given in Appendix D.

Calculations of Poynting's vector in each medium show that the transmission and reflection coefficients through the antiferromagnetic film are

$$T = \frac{\epsilon_1}{\epsilon_3}\frac{|t|^2}{|p|^2}, \quad (31)$$

$$R = \frac{|r|^2}{|p|^2} \quad (32)$$

for linear waves and

$$\mathcal{T} = \frac{\epsilon_1}{\epsilon_3}\frac{|\tau|^2}{|p|^2}, \quad (33)$$

$$\mathcal{R} = \frac{|\rho|^2}{|p|^2} \tag{34}$$

for SH waves, where ϵ_1 and ϵ_3 are the dielectric constants for media 1 and 3, respectively, that sandwich the antiferromagnetic film. The coefficient for the amplitude of input waves is p, and $|p|^2$ is directly proportional to input power I_p, where

$$I_p = \frac{1}{2}\frac{k_1}{\epsilon_0 \epsilon \omega}|p|^2. \tag{35}$$

5. RESULTS AND DISCUSSION

The transmission and reflection coefficients in Section 4, Eqs. (31)–(34), have been shown graphically by use of the parameters of FeF_2, which is a simple two-sublattice antiferromagnet. These parameters are $\epsilon = 5.5$ for the dielectric constant, $\gamma/\mu_0 = 1.05\ \mathrm{cm^{-1}\ T^{-1}}$ for the gyromagnetic ratio, $\mu_0 H_E = 53.3$ T for the exchange field, $\mu_0 H_A = 19.7$ T for the anisotropy field, $\mu_0 M_0 = 0.056$ T for the sublattice magnetization, and $\mu_0 H_0$ for the applied static field. In the calculations the chosen damping parameter[4] is $\eta = 5 \times 10^{-4}$. The linear and SH transmission and reflection coefficients are plotted in Figs. 3 and 4 versus frequency sweep with various fixed values of thickness and applied static fields. Figure 5 shows the linear and SH transmission and reflection coefficients versus thickness for $\mu_0 H_0 = 3$ T and input frequency $\omega = 55\ \mathrm{cm^{-1}}$. The input intensity that produced the results in Figs. 3–5 is $I_p = 1.6 \times 10^{15}\ \mathrm{W\ m^{-2}}$. If the far infrared is focused to a 0.5-$\mathrm{mm^2}$ beam, the strength of field H is approximately 18 G and is currently achievable.[5]

From Fig. 3, linear transmission and reflection show clearly that there are two antiferromagnetic resonances for x-polarized input waves in the presence of static applied magnetic field $\mu_0 H_0$. This is expected from the mathematical expressions for the linear susceptibility of x-polarized waves, χ_{xx}, as given in Eq. (8), because x-polarized waves are superpositions of two circularly polarized waves, and the resonances for these two circular waves are split in a nonzero applied static field, as implied by the susceptibility elements of these circular waves, χ_{pp} and χ_{nn}, in Appendix A. From Appendix A it can be seen that the resonance for a p-circular wave will occur at frequency $\omega_p = \omega_R - \omega_0$, whereas the resonance for an n-circular wave will occur at $\omega_n = \omega_R + \omega_0$, where ω_R is the resonance frequency for the antiferromagnet and $\omega_0 = \gamma H_0$ is the frequency shift that is due to applied static field $\mu_0 H_0$. For FeF_2, $\omega_R = 52.4\ \mathrm{cm^{-1}}$, and for 3 and 6 T of the applied static field the gap between the p resonance and the n resonance, $\omega_g = 2\omega_0$, will be 6.3 and 12.6 $\mathrm{cm^{-1}}$, as shown clearly in Figs. 3(a) and 3(c) and Figs. 3(b) and 3(d), respectively. The dips at resonance for both transmission and reflection curves are due to the strong antiferromagnetic absorption at the resonance frequencies, whereas the peaks and troughs away from resonance are due to the dimensional resonance that depends on wave vector k_V and on the film thickness L.

The SH transmission and reflection are ~2 orders weaker than the linear transmission and reflection, and $\mathcal{T}$ and $\mathcal{R}$ are significant only in the vicinities of antiferromagnetic resonances. From the curves shown in Figs. 4 and 5 and the model shown schematically in Fig. 2, it is obvious that the peaks and troughs of the SH transmission reflection curves not only are due to the antiferromagnetic and dimensional resonance but also are affected by the input resonance (standing waves in the films that generate T) and the output resonance (standing waves in the films that generate R) of the linear waves. With all these resonance enhancements, the signals shown in $\mathcal{T}$ and $\mathcal{R}$ would not be regular peaks and troughs similarly to linear transmission and reflection but somehow irregular, especially in the vicinities of the antiferromagnetic resonances. These enhancements are shown clearly in Figs. 4 and 5(b), which compare the existence of $\mathcal{T}$ and $\mathcal{R}$ peaks to that of the peaks of linear transmission in Figs. 3 and 5(a).

In the usual nonlinear optics, SHG signals are significant when phase-matching occurs. In terms of the methodology described this paper, linear susceptibilities χ_{xx} and χ_{xy} are complex quantities, whereas $\chi_{zz} = 0$. k_z is proportional to $\sqrt{1 + \chi_{zz}}$, and therefore it is real, whereas k_V depends on χ_{xx} and χ_{xy} and basically is a complex quantity. The condition for phase matching is that $k_z = 2k_V$. Therefore there is no chance to achieve phase matching for the AFM films. In particular, the input waves have frequencies in the vicinity of linear AFM resonances for which the imaginary parts of χ_{xx} and χ_{xy} are significant. The peaks and troughs in $\mathcal{T}$ and $\mathcal{R}$ can be described as the pseudo-phase matching that occurs when one or more of the resonance enhancements described above occurs. Another important property of SH transmission and reflection is that $\mathcal{T}$ and $\mathcal{R}$ have no phase difference if they are compared to linear transmission and reflection with a $\pi/2$ phase difference. The reason for this is that the SH output, $\mathcal{T}$ and $\mathcal{R}$, has no input from the medium at the left of an antiferromagnetic film, as for the linear case. The only difference between $\mathcal{T}$ and $\mathcal{R}$ is in terms of magnitudes: $\mathcal{T}$ is greater than $\mathcal{R}$ because the input resonance that affects $\mathcal{T}$ directly is stronger than the output resonance.

6. CONCLUSIONS

The main results of this paper have been the calculation and formulation of terms that describe the generation of SH waves through an antiferromagnetic film based entirely on the magnetic response of an antiferromagnet rather than on magneto-optical effects based electrical responses that are affected by the existence of magnetization.[9,10] The calculations here have made use of the conventional approach in which, for weak nonlinearity, only 1–2% of the input intensity is converted to SH waves and therefore the assumption of no depletion of the input waves has been used to simplify the calculation. However, the approach that has been used here varies slightly from the usual formulation in nonlinear optics in that we have neglected the slowly varying envelope approximation.[11]

The approach that was used here may facilitate using such methods as the conventional nonlinear optics approach to study and characterize nonlinear effects and their applications in magnetic systems. The results

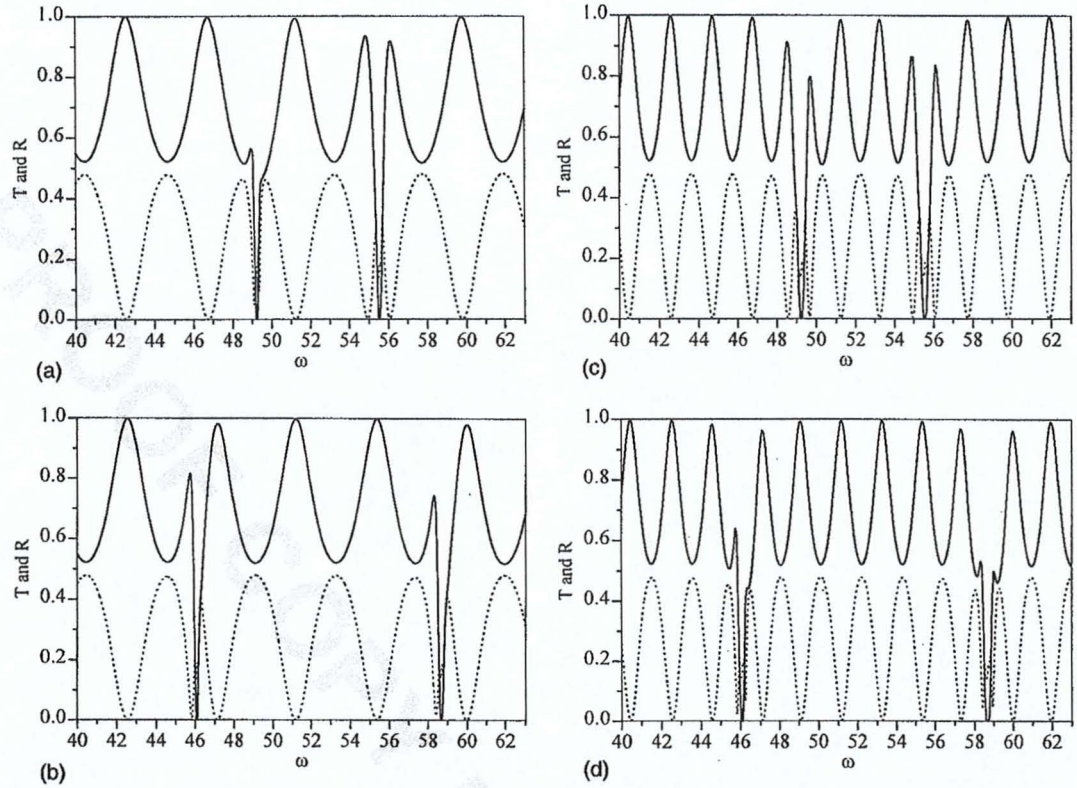

Fig. 3. Linear transmission T (solid curves) and reflection R (dashed curves) for two thicknesses L and two applied static magnetic fields $\mu_0 H_0$ versus frequency sweep ω (in inverse centimeters). (a) $L = 0.5$ mm, $\mu_0 H_0 = 3.0$ T; (b) $L = 0.5$ mm, $\mu_0 H_0 = 6.0$ T; (c) $L = 1.0$ mm, $\mu_0 H_0 = 3.0$ T; (d) $L = 1.0$ mm, $\mu_0 H_0 = 6.0$ T.

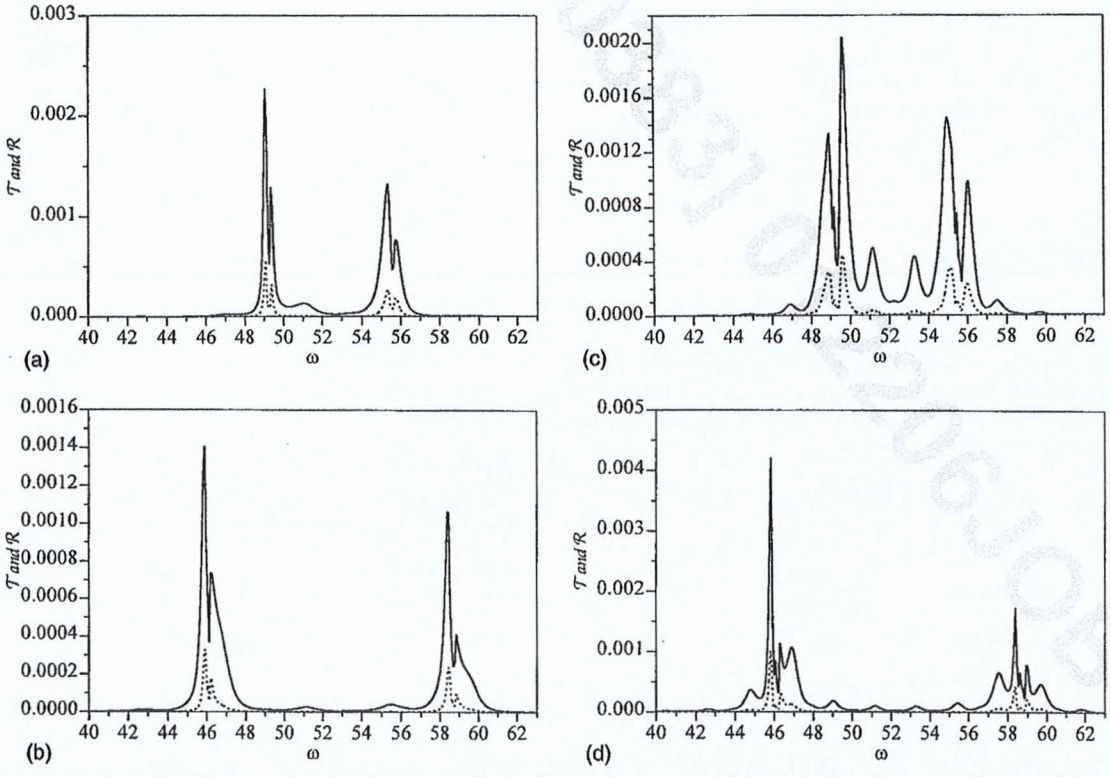

Fig. 4. SH transmission $\mathcal{T}$ (solid curves) and reflection $\mathcal{R}$ (dashed curves) for two thicknesses L and two applied static magnetic fields $\mu_0 H_0$ versus frequency sweep $\Omega/2$ (in inverse centimeters). (a) $L = 0.5$ mm, $\mu_0 H_0 = 3.0$ T; (b) $L = 0.5$ mm, $\mu_0 H_0 = 6.0$ T; (c) $L = 1.0$ mm, $\mu_0 H_0 = 3.0$ T; (d) $L = 1.0$ mm, $\mu_0 H_0 = 6.0$ T.

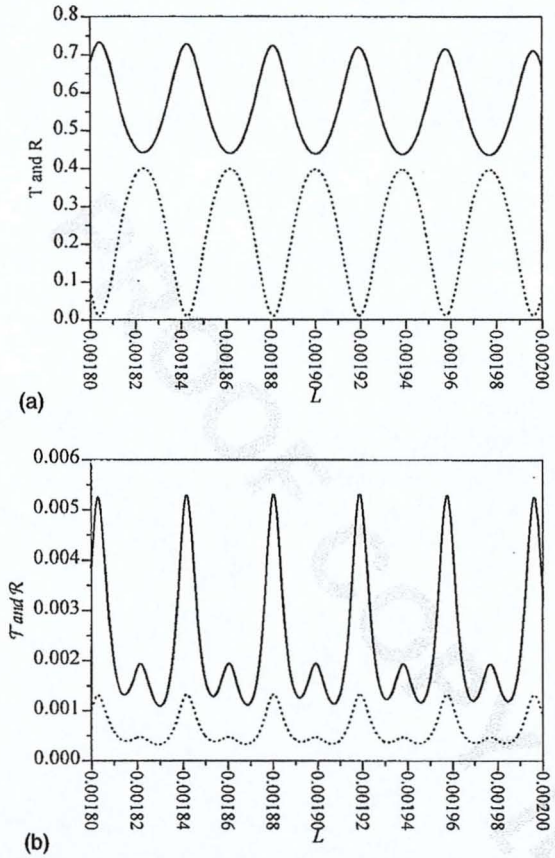

Fig. 5. Transmission (solid curves) and reflection (dashed curves) for (a) linear waves and (b) SH waves versus thickness with input frequency $\omega = 55.0\ \mathrm{cm}^{-1}$ and applied static magnetic field $\mu_0 H_0 = 3.0$ T.

shown in Sections 3–5 were expected from the approaches that were used and may be extrapolated to more-sophisticated cases such as the generation of SH waves with the depletion of input waves, and the systems may be extended to include magnetic superlattices.

APPENDIX A. INDEPENDENT NONVANISHING LINEAR AND SECOND-HARMONIC SUSCEPTIBILITY ELEMENTS IN A (p, n, z) SYSTEM

The complete mathematical expressions for the independent nonvanishing linear and nonlinear elements up to SH effects in a circular polarization system (p, n, z) are given. The linear p elements are

$$\chi_{pp}^{\lambda} = r_{1p}\{(1+\eta^2)\omega_E + (1+i\eta)[\omega - (1 - i\eta)\omega_v]\}\omega_m, \qquad \omega_v = \gamma(H_E + H_A - H_0), \tag{A1}$$

$$\chi_{pp}^{v} = r_{1p}\{(1+\eta^2)\omega_E - (1-i\eta)[\omega + (1 + i\eta)\omega_\lambda]\}\omega_m, \qquad \omega_\lambda = \gamma(H_E + H_A + H_0), \tag{A2}$$

$$\chi_{pp} = r_{1p}[-2\omega_m\omega_A(1+\eta^2) + i2\eta\omega\omega_m], \tag{A3}$$

where

$$r_{1p} = [\omega^2 + 2\omega\omega_0 + (\omega_0^2 - \omega_R^2)(1+\eta^2) + i2\eta\omega(\omega_E + \omega_A)]^{-1}. \tag{A4}$$

The linear elements n are

$$\chi_{nn}^{\lambda} = r_{1n}\{(1+\eta^2)\omega_E - (1-i\eta)[\omega + (1+i\eta)\omega_v]\}\omega_m, \tag{A5}$$

$$\chi_{nn}^{v} = r_{1n}\{(1+\eta^2)\omega_E + (1+i\eta) \times [\omega - (1-i\eta)\omega_\lambda]\}\omega_m, \tag{A6}$$

$$\chi_{nn} = r_{1n}[-2\omega_m\omega_A(1+\eta^2) + i2\eta\omega\omega_m], \tag{A7}$$

where

$$r_{1n} = [\omega^2 - 2\omega\omega_0 + (\omega_0^2 - \omega_R^2)(1+\eta^2) + i2\eta\omega(\omega_E + \omega_A)]^{-1}. \tag{A8}$$

The SH p, n, and z elements are

$$\chi_{ppz} = \tfrac{1}{2}\gamma r_{2p}[-2\omega(\chi_{pp}^{\alpha} + \chi_{pp}^{\beta}) + (\omega_E + i\eta 2\omega) \times (\chi_{pp}^{\beta} - \chi_{pp}^{\alpha}) + (1+\eta^2)(\omega_\beta\chi_{pp}^{\alpha} - \omega_\alpha\chi_{pp}^{\beta})], \tag{A9}$$

$$\chi_{nnz} = \tfrac{1}{2}\gamma r_{2n}[2\omega(\chi_{nn}^{\alpha} + \chi_{nn}^{\beta}) + (\omega_E + i\eta 2\omega) \times (\chi_{nn}^{\beta} - \chi_{nn}^{\alpha}) + (1+\eta^2)(\omega_\beta\chi_{nn}^{\alpha} - \omega_\alpha\chi_{nn}^{\beta})], \tag{A10}$$

$$\chi_{zpn} = \frac{1}{2\omega}[(1+i\eta)\gamma(\chi_{pp}^{v} - \chi_{nn}^{\lambda}) + (1-i\eta)\gamma(\chi_{pp}^{\lambda} - \chi_{nn}^{v}) + (i2\eta/M_0) \times (\omega_\lambda\chi_{pp}^{\lambda}\chi_{nn}^{\lambda} - \omega_v\chi_{pp}^{v}\chi_{nn}^{v})], \tag{A11}$$

where

$$r_{2p} = [4\omega^2 + 4\omega\omega_0 + (\omega_0^2 - \omega_R^2)(1+\eta^2) + i4\eta\omega(\omega_E + \omega_A)]^{-1}, \tag{A12}$$

$$r_{2n} = [4\omega^2 - 4\omega\omega_0 + (\omega_0^2 - \omega_R^2)(1+\eta^2) + i4\eta\omega(\omega_E + \omega_A)]^{-1}, \tag{A13}$$

where $\omega_E = \gamma H_E$, $\omega_A = \gamma H_A$, $\omega_m = \gamma M_0$, $\omega_0 = \gamma H_0$, $\omega_\alpha = \gamma H_\alpha$, and $\omega_R = (2\omega_A\omega_E + \omega_A^2)^{1/2}$. H_E is the exchange field, H_A is the anisotropy field, and $\gamma = -g\mu_B\mu_0$ is the gyromagnetic ratio. The complete nonvanishing elements are obtained by use of intrinsic permutation symmetry.

APPENDIX B. CALCULATIONS OF LINEAR AND SECOND-HARMONIC WAVES IN VOIGT GEOMETRY

We consider Maxwell's equations in nonconducting magnetic materials:

$$\nabla \times \mathbf{E} = -\frac{\partial \mathbf{B}}{\partial t}, \tag{B1}$$

$$\nabla \times \mathbf{H} = \frac{\partial \mathbf{D}}{\partial t}, \tag{B2}$$

$$\nabla \cdot \mathbf{B} = 0, \tag{B3}$$

$$\nabla \cdot \mathbf{D} = 0, \tag{B4}$$

$$\mathbf{D} = \epsilon_0(\mathbf{E} + \mathbf{P}) = \epsilon_0\epsilon\mathbf{E}, \tag{B5}$$

$$\mathbf{B} = \mu_0(\mathbf{H} + \mathbf{M}). \tag{B6}$$

For an antiferromagnetic material such as FeF_2, $\epsilon = 1 + \chi_e$ is a constant with respect to the applied static magnetic field and the frequency range of interest (the far infrared).

For an x-polarized wave with single frequency ω incident in the y direction as shown in Fig. 2,

$$H_x(y, t) = \tfrac{1}{2}H_{x0}(y)\exp(-i\omega t) + \text{c.c.} \tag{B7}$$

At first sight, we may conclude that the effective linear susceptibility elements are χ_{xx} and χ_{yx} only. However, the induced rf magnetization that is due to χ_{yx} is y polarized and will always counterinduce a y-polarized rf magnetic field in the film:

$$H_y(y, t) = \tfrac{1}{2}H_{y0}(y)\exp(-i\omega t) + \text{c.c.}, \tag{B8}$$

so the transverse nature of the electromagnetic waves, i.e., Eqs. (B1)–(B4), is conserved in the antiferromagnetic film. Therefore the effective linear and SH susceptibility elements are χ_{xx}, χ_{xy}, χ_{yx}, χ_{yy}, χ_{zxx}, and χ_{zyy}. The induced linear magnetizations are

$$M_x^{(1)}(y, t) = \tfrac{1}{2}[\chi_{xx}H_{x0}(y) + \chi_{xy}H_{y0}(y)] \times \exp(-i\omega t) + \text{c.c.}, \tag{B9}$$

$$M_y^{(1)}(y, t) = \tfrac{1}{2}[\chi_{yx}H_{x0}(y) + \chi_{yy}H_{y0}(y)] \times \exp(-i\omega t) + \text{c.c.}, \tag{B10}$$

and the induced SH magnetization is

$$M_z^{(2)}(y, t) = \tfrac{1}{2}K_{2\omega}^{(2)}[\chi_{zxx}H_{x0}(y)H_{x0}(y) + \chi_{zyy}H_{y0}(y)H_{y0}(y)]\exp(-i\Omega t) + \text{c.c.}, \tag{B11}$$

where $\Omega = 2\omega$. From Eq. (B6), the corresponding linear and SH magnetic inductions are

$$B_x^{(1)}(y, t) = \tfrac{1}{2}\mu_0[H_{x0}(y) + \chi_{xx}H_{x0}(y) + \chi_{xy}H_{y0}(y)]\exp(-i\omega t) + \text{c.c.}, \tag{B12}$$

$$B_y^{(1)}(y, t) = \tfrac{1}{2}\mu_0[H_{y0}(y) + \chi_{yx}H_{x0}(y) + \chi_{yy}H_{y0}(y)]\exp(-i\omega t) + \text{c.c.}, \tag{B13}$$

$$B_z^{(2)}(y, t) = \tfrac{1}{2}\mu_0[H_{z0}(y) + K_{2\omega}^{(2)}\chi_{zxx}H_{x0}(y)H_{x0}(y) + K_{2\omega}^{(2)}\chi_{zyy}H_{y0}(y)H_{y0}(y)] \times \exp(-i\Omega t) + \text{c.c.} \tag{B14}$$

For waves propagating along the y direction the magnetic film is extended infinitely in the xz plane:

$$\nabla \to \hat{y}\frac{\partial}{\partial y}, \qquad \nabla^2 \to \frac{\partial^2}{\partial y^2}. \tag{B15}$$

From the third Maxwell equation, $\nabla \cdot \mathbf{B} = 0$, the magnetic induction is tranverse to the direction of propagation. To satisfy this condition $B_y^{(1)}(y, t)$ must be equal to zero, or

$$H_{y0}(y) + \chi_{yx}H_{x0}(y) + \chi_{yy}H_{y0}(y) = 0. \tag{B16}$$

From Eqs. (8), (9), and (B16), the conclusion is that $H_y^{(1)}(y, t)$ propagates collinearly with $H_x^{(1)}(y, t)$:

$$H_{y0}(y) = \frac{\mu_{xy}}{\mu_{xx}}H_{x0}(y), \tag{B17}$$

where $\mu_{xx} = \mu_{yy} = 1 + \chi_{xx}$ and $\mu_{xy} = -\mu_{yx} = \chi_{xy}$. Substituting Eq. (B17) into Eqs. (B12) and (B14) yields

$$B_x^{(1)}(y, t) = \tfrac{1}{2}\mu_0\mu_V H_{x0}(y)\exp(-i\omega t) + \text{c.c.}, \tag{B18}$$

$$B_z^{(2)}(y, t) = \tfrac{1}{2}\mu_0[H_{z0}(y) - \bar{\Gamma}H_{x0}(y)H_{x0}(y)] \times \exp(-i\Omega t) + \text{c.c.}. \tag{B19}$$

where

$$\mu_V = \mu_{xx} + \frac{(\mu_{xy})^2}{\mu_{xx}}, \tag{B20}$$

$$\bar{\Gamma} = -K_{2\omega}^{(2)}[1 + (\mu_{xy}/\mu_{xx})^2]\chi_{zxx}. \tag{B21}$$

To derive linear and SH wave propagation in Voigt geometry, let us take the curl of Eq. (B2). Using the identity of vector products, Eqs. (B1) and (B5), yields

$$\nabla(\nabla \cdot \mathbf{H}) - (\nabla \cdot \nabla)\mathbf{H} = -\epsilon_0\epsilon\frac{\partial^2\mathbf{B}}{\partial t^2}. \tag{B22}$$

By use of Eqs. (B7) and (B8), relation (B15), and Eqs. (B16)–(B21), Eq. (B22) can be split into two wave equations, for x-polarized and z-polarized rf magnetic fields:

$$\frac{\partial^2 H_{x0}(y)}{\partial y^2} + k_V^2 H_{x0}(y) = 0, \tag{B23}$$

$$\frac{\partial^2 H_{z0}(y)}{\partial y^2} + k_z^2 H_{z0}(y) = \Gamma H_{x0}(y)H_{x0}(y), \tag{B24}$$

respectively, where

$$K_V^2 = \omega^2\epsilon_0\mu_0\epsilon\mu_V, \tag{B25}$$

$$k_z^2 = \Omega^2\epsilon_0\mu_0\epsilon, \tag{B26}$$

$$\Gamma = \epsilon_0\mu_0\epsilon\Omega^2\bar{\Gamma}. \tag{B27}$$

The general solution for x-polarized wave equation (B23) is

$$H_{x0}(y) = a\exp(ik_V y) + b\exp(-ik_V y), \tag{B28}$$

where a and b are to be determined with the boundary conditions of the film. The complete expression with time dependence is

$$H_x(y, t) = \tfrac{1}{2}H_{x0}(y)\exp(-i\omega t) + \text{c.c.} = \tfrac{1}{2}[a\exp(ik_V y) + b\exp(-ik_V y)] \times \exp(-i\omega t) + \text{c.c.} \tag{B29}$$

From Eq. (B2), the rf electric fields are related to the rf magnetic field as

$$\epsilon_0\epsilon\frac{\partial E_z}{\partial t} = -\frac{\partial H_x}{\partial y}, \tag{B30}$$

$$\epsilon_0\epsilon\frac{\partial E_x}{\partial t} = \frac{\partial H_z}{\partial y}. \tag{B31}$$

Therefore the corresponding linear rf electric field related to $H_{x0}(y, t)$ is

$$E_z(y, t) = \frac{1}{2}\frac{k_V}{\epsilon_0\epsilon\omega}[a\exp(ik_V y) - b\exp(-ik_V y)]\exp(-i\omega t) + \text{c.c.} \tag{B32}$$

Equations (B28), (B29), and (B32) allow the waves to propagate in both positive and negative directions, i.e., in a film.

Equation (B24) is a linear, inhomogeneous second-order differential equation for $H_{z0}(y)$. It has a source term that depends on the solution of $H_{x0}(y)$ in Eq. (B28). The complete SH wave equation for the z-polarized rf magnetic field is

$$\frac{\partial^2 H_{z0}(y)}{\partial y^2} + k_z{}^2 H_{z0}(y) = \Gamma[a^2\exp(i\xi y) + b^2\exp(-i\xi y) + 2ab], \tag{B33}$$

where $\xi = 2k_V$. The homogeneous solution for Eq. (B33) is

$$H_{z0h}(y) = \alpha\exp(ik_z y) + \beta\exp(-ik_z y), \tag{B34}$$

where α and β are determined with appropriate boundary conditions. The particular solution for Eq. (B33) depends on the condition $k_z \neq \xi$ (phase mismatch) or $k_z = \xi$ (phase matching).

For $k_z \neq \xi$ (phase mismatch), the particular solution for Eq. (B33) is

$$H_{z0p}(y) = f_1\exp(i\xi y) + f_2\exp(-i\xi y) + f_3, \tag{B35}$$

where

$$f_1 = \frac{\Gamma a^2}{(k_z{}^2 - \xi^2)}, \qquad f_2 = \frac{\Gamma b^2}{(k_z{}^2 - \xi^2)}, \qquad f_3 = \frac{2ab\Gamma}{k_z{}^2}. \tag{B36}$$

The general solutions for Eq. (B33) have the form

$$H_{z0}(y) = \alpha\exp(ik_z y) + \beta\exp(-ik_z y) + f_1\exp(i\xi y) + f_2\exp(-i\xi y) + f_3, \tag{B37}$$

and, with the inclusion of time dependence,

$$H_z(y, t) = \tfrac{1}{2}[\alpha\exp(ik_z y) + \beta\exp(-ik_z y) + f_1\exp(i\xi y) + f_2\exp(-i\xi y) + f_3]\exp(-i\Omega t) + \text{c.c.} \tag{B38}$$

The E field related to $H_z(y, t)$ is given by Eq. (B31):

$$\epsilon_0\epsilon\frac{\partial E_x}{\partial t} = \frac{\partial H_z}{\partial y}.$$

Therefore

$$E_x(y, t) = \frac{1}{2}\frac{1}{\epsilon_0\epsilon\Omega}[-\alpha k_z\exp(ik_z y) + \beta k_z\exp(-ik_z y) - f_1\xi\exp(i\xi y) + f_2\xi\exp(-i\xi y)] \times \exp(-i\Omega t) + \text{c.c.} \tag{B39}$$

For $k_z = \xi$ (phase matching) the particular solution for Eq. (B33) is

$$H_{z0p}(y) = yd_1\exp(i\xi y) + yd_2\exp(-i\xi y) + d_3, \tag{B40}$$

where

$$d_1 = \frac{\Gamma a^2}{i2\xi}, \qquad d_2 = \frac{\Gamma b^2}{-i2\xi}, \qquad d_3 = \frac{2ab\Gamma}{\xi^2}. \tag{B41}$$

The general solutions for Eq. (B33) have the forms

$$H_{z0}(y) = \alpha\exp(i\xi y) + \beta\exp(-i\xi y) + yd_1\exp(i\xi y) + yd_2\exp(-i\xi y) + d_3, \tag{B42}$$

and, with time dependence,

$$H_z(y, t) = \tfrac{1}{2}[(\alpha + yd_1)\exp(i\xi y) + (\beta + yd_2) \times \exp(-i\xi y) + d_3]\exp(-i\Omega t) + \text{c.c.} \tag{B43}$$

Again, the E field related to $H_z(y, t)$ is given by Eq. (B31):

$$E_x(y, t) = \frac{1}{2}\frac{1}{\epsilon_0\epsilon\Omega}[(-\alpha\xi + id_1 - \xi y d_1)\exp(i\xi y) + (\beta\xi + id_2 + \xi y d_2)\exp(-i\xi y)] \times \exp(-i\Omega t) + \text{c.c.} \tag{B44}$$

APPENDIX C. LINEAR AMPLITUDE TRANSMISSION AND REFLECTION OF AN ANTIFERROMAGNETIC FILM IN VOIGT GEOMETRY

To calculate $\mathcal{R}$ and $\mathcal{T}$ for the SHG of an antiferromagnetic film we have to solve the coefficients of a linear wave equation, a and b, in the film and use the results for formation of a SHG wave. For a magnetic film in Voigt geometry, a schematic diagram simplified from Fig. 2 for the linear wave is shown in Fig. 6. In Fig. 6, p, r, and t represent the amplitude coefficients for incident, reflection, and transmission angles, respectively.

From Appendix B, the dynamic magnetic and electric fields in medium 1 are

$$H_x = \tfrac{1}{2}[p\exp(ik_1 y) + r\exp(-ik_1 y)]\exp(-i\omega t) + \text{c.c.}, \tag{C1}$$

$$E_z = \frac{1}{2}\frac{k_1}{\epsilon_0\epsilon_1\omega}[p\exp(ik_1 y) - r\exp(-ik_1 y)]\exp(-i\omega t) + \text{c.c.}, \tag{C2}$$

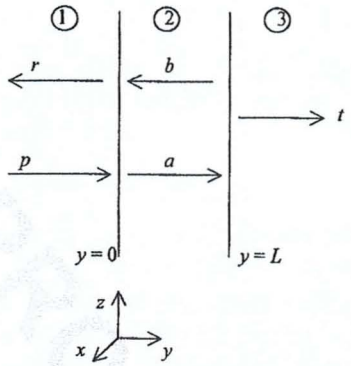

Fig. 6. Schematic diagram for transmission and reflection of linear waves.

$$k_1^2 = \omega^2 \epsilon_0 \mu_0 \epsilon_1 . \tag{C3}$$

The dynamic magnetic and electric fields in medium 2 are

$$H_x = \tfrac{1}{2}[a \exp(ik_V y) + b \exp(-ik_V y)]\exp(-i\omega t) + \text{c.c.}, \tag{C4}$$

$$E_z = \frac{1}{2}\frac{k_V}{\epsilon_0 \epsilon \omega}[a \exp(ik_V y) - b \exp(-ik_V y)]\exp(-i\omega t) + \text{c.c.} \tag{C5}$$

The dynamic magnetic and electric fields in medium 3 are

$$H_x = \tfrac{1}{2}[t \exp(ik_3 y) + O \exp(-ik_3 y)]\exp(-i\omega t) + \text{c.c.} \tag{C6}$$

$$E_z = \frac{1}{2}\frac{k_3}{\epsilon_0 \epsilon_3 \omega}[t \exp(ik_3 y) - O \exp(-ik_3 y)]\exp(-i\omega t) + \text{c.c.}, \tag{C7}$$

$$k_3^2 = \omega^2 \epsilon_0 \mu_0 \epsilon_3 . \tag{C8}$$

From electromagnetic theory, the tangential components for the magnetic and the electric fields are conserved across the boundary. Therefore the amplitude coefficients for the three media are related as

$$p + r = a + b, \tag{C9}$$

$$q_1(p - r) = q_V(a - b), \tag{C10}$$

$$a\delta + b\delta^{-1} = t\theta, \tag{C11}$$

$$q_V(a\delta - b\delta^{-1}) = q_3 t\theta, \tag{C12}$$

where $\delta = \exp(ik_V L)$, $\theta = \exp(ik_3 L)$, $q_V = k_V/\epsilon$, and $q_i = k_i/\epsilon_i$. Coefficients a, b, r, and t can be solved in terms of p, ϵ_i, and k_i. The solutions for these coefficients are

$$a = \frac{2q_1(q_V + q_3)p}{(q_1 + q_V)(q_V + q_3) + (q_1 - q_V)(q_V - q_3)\delta^2}, \tag{C13}$$

$$b = \frac{2q_1(q_V - q_3)\delta^2 p}{(q_1 + q_V)(q_V + q_3) + (q_1 - q_V)(q_V - q_3)\delta^2}, \tag{C14}$$

$$r = a + b - p, \tag{C15}$$

$$t = \theta^{-1}(a\delta + b\delta^{-1}). \tag{C16}$$

APPENDIX D. SECOND-HARMONIC AMPLITUDE TRANSMISSION AND REFLECTION OF AN ANTIFERROMAGNETIC FILM IN VOIGT GEOMETRY

SH transmission and reflection depend on amplitude coefficients a and b calculated in Appendix C. A schematic diagram of the SH wave is shown in Fig. 7. The dynamic magnetic and electric fields in medium 1 are

$$H_z = \tfrac{1}{2}\rho \exp(-i\bar{k}_1 y)\exp(-i\Omega t) + \text{c.c.}, \tag{D1}$$

$$E_x = \frac{1}{2}\frac{\bar{k}_1}{\epsilon_0 \epsilon_1 \Omega}\rho \exp(-i\bar{k}_1 y)\exp(-i\Omega t) + \text{c.c.}, \tag{D2}$$

$$\bar{k}_1^2 = \Omega^2 \epsilon_0 \mu_0 \epsilon_1 . \tag{D3}$$

For phase mismatch, $k_z \neq 2k_V = \xi$, the dynamic magnetic and electric fields in medium 2 are

$$H_z = \tfrac{1}{2}[\alpha \exp(ik_z y) + \beta \exp(-ik_z y) + f_1 \exp(i\xi y) + f_2 \exp(-i\xi y) + f_3]\exp(-i\Omega t) + \text{c.c.}, \tag{D4}$$

$$E_x = \frac{1}{2}\frac{1}{\epsilon_0 \epsilon \Omega}[-\alpha k_z \exp(ik_z y) + \beta k_z \exp(-ik_z y) - f_1 \xi \exp(i\xi y) + f^2 \xi \exp(-i\xi y)]\exp(-i\Omega t) + \text{c.c.} \tag{D5}$$

However, for phase matching, $k_z = 2k_V = \xi$, the dynamic magnetic and electric fields in medium 2 are

$$H_z = \tfrac{1}{2}[(\alpha + yd_1)\exp(i\xi y) + (\beta + yd_2)\exp(-i\xi y) + d_3]\exp(-i\Omega t) + \text{c.c.}, \tag{D6}$$

$$E_x = \frac{1}{2}\frac{1}{\epsilon_0 \epsilon \Omega}[(-\alpha\xi + id_1 - \xi y d_1)\exp(i\xi y) + (\beta\xi + id_2 + \xi y d_2)\exp(-i\xi y)]\exp(-i\Omega t) + \text{c.c.} \tag{D7}$$

The dynamic magnetic and electric fields in medium 3 are

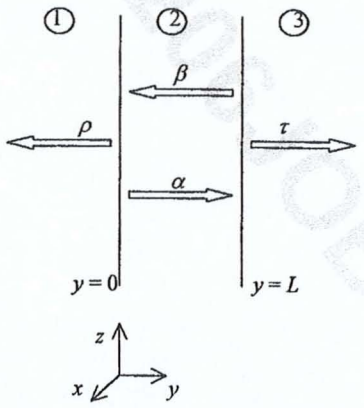

Fig. 7. Schematic diagram for transmission and reflection of SH waves.

$$H_z = \tfrac{1}{2}\tau \exp(i\bar{k}_3 y)\exp(-i\Omega t) + \text{c.c.}, \tag{D8}$$

$$E_x = -\frac{1}{2}\frac{\bar{k}_3}{\epsilon_0 \epsilon_3 \Omega}\tau \exp(i\bar{k}_3 y)\exp(-i\Omega t) + \text{c.c.}, \tag{D9}$$

$$k_3{}^2 = \Omega^2 \epsilon_0 \mu_0 \epsilon_3 . \tag{D10}$$

Applying boundary conditions yields

$$\rho = \alpha + \beta + \phi_{\text{hl}}, \tag{D11}$$

$$\eta_1 \rho = -\alpha \eta_z + \beta \eta_z + \phi_{\text{el}}, \tag{D12}$$

$$\alpha\Delta + \beta\Delta^{-1} + \phi_{\text{hr}} = \tau\Pi, \tag{D13}$$

$$-\alpha\eta_z\Delta + \beta\eta_z\Delta^{-1} + \phi_{\text{er}} = -\eta_3\tau\Pi, \tag{D14}$$

where $\Delta = \exp(ik_z L)$, $\Theta = \exp(i\xi L)$, $\Pi = \exp(i\bar{k}_3 L)$, $\eta_1 = \bar{k}_1/\epsilon_1$, $\eta_3 = \bar{k}_3/\epsilon_3$, $\eta_z = k_z/\epsilon$, and $\eta_V = \xi/\epsilon$.

The solutions for α, β, τ, and ρ are

$$\alpha = \frac{(\eta_z + \eta_3)(\phi_{\text{el}} - \eta_1\phi_{\text{hl}})\Delta^{-1} + (\eta_1 - \eta_z)(\phi_{\text{er}} + \eta_3\phi_{\text{hr}})}{(\eta_1 + \eta_z)(\eta_z + \eta_3)\Delta^{-1} - (\eta_1 - \eta_z)(\eta_3 - \eta_z)\Delta}, \tag{D15}$$

$$\beta = \frac{-(\eta_1 + \eta_z)(\phi_{\text{er}} + \eta_3\phi_{\text{hr}}) - (\eta_3 - \eta_z)(\phi_{\text{el}} - \eta_1\phi_{\text{hl}})\Delta}{(\eta_1 + \eta_z)(\eta_z + \eta_3)\Delta^{-1} - (\eta_1 - \eta_z)(\eta_3 - \eta_z)\Delta}, \tag{D16}$$

$$\rho = \alpha + \beta + \phi_{\text{hl}}, \tag{D17}$$

$$\tau = (\alpha\Delta + \beta\Delta^{-1} + \phi_{\text{hr}})\Pi^{-1}, \tag{D18}$$

where $\phi_{\text{ij}} = U_{\text{ij}}$ for phase mismatching and $\phi_{\text{ij}} = V_{\text{ij}}$ for phase matching. The explicit expressions for U_{ij} and V_{ij} are

$$U_{\text{hl}} = f_1 + f_2 + f_3, \tag{D19}$$

$$U_{\text{el}} = f_1\eta_V + f_2\eta_V, \tag{D20}$$

$$U_{\text{hr}} = f_1\Theta + f_2\Theta^{-1} + f_3, \tag{D21}$$

$$U_{\text{er}} = -f_1\eta_V\Theta + f_2\eta_V\Theta^{-1}, \tag{D22}$$

$$V_{\text{hl}} = d_3, \tag{D23}$$

$$V_{\text{el}} = \frac{i(d_1 + d_2)}{\epsilon}, \tag{D24}$$

$$V_{\text{hr}} = d_1 L\Theta + d_2 L\Theta^{-1} + d_3, \tag{D25}$$

$$V_{\text{er}} = -\eta_V L d_1\Theta + \eta_V L d_2\Theta^{-1} + \frac{i(d_1\Theta + d_2\Theta^{-1})}{\epsilon}. \tag{D26}$$

ACKNOWLEDGMENT

The author thanks D. R. Tilley for valuable and helpful discussions. This study was supported by a research grant provided by Universiti Sains Malaysia, Penang, Malaysia.

The author's e-mail address is limsiewchoo1 @yahoo.com.

REFERENCES

1. P. N. Butcher and D. Cotter, *The Elements of Nonlinear Optics* (Cambridge U. Press, Cambridge, 1990), pp. 5, 211–226.
2. D. L. Mills, *Nonlinear Optics*, 2nd ed. (Springer, New York, 1998), p. 5.
3. S. C. Lim, J. Osman, and D. R. Tilley, "Calculation of nonlinear magnetic susceptibility tensors for a ferromagnet," J. Phys. D **32**, 755–763 (1999).
4. S. C. Lim, J. Osman, and D. R. Tilley, "Calculation of nonlinear magnetic susceptibility tensors for a uniaxial antiferromagnet," J. Phys. D **33**, 2899–2910 (2000).
5. N. S. Almeida and D. L. Mills, "Nonlinear infrared response of antiferromagnet," Phys. Rev. B **36**, 2015–2023 (1987).
6. S. Vukovich, S. N. Gavrilin, and S. A. Nikitov, "Nonlinear electromagnetic waves in an antiferromagnetic plate subjected to an external magnetic field," Sov. Phys. JETP **71**, 964–968 (1990).
7. D. Frohlich, Th. Kiefer, St. Leute, and Th. Lottermoser, "Nonlinear spectroscopy of antiferromagnet," Appl. Phys. B **68**, 465–471 (1999).
8. K. Abraha and D. R. Tilley, "Theory of far infrared properties of magnetic surfaces, films and superlattices," Surf. Sci. Rep. **24**, 125–222 (1996).
9. Y. Z. Wu, R. Vollmer, H. Regensburger, X. F. Jin, and J. Kirschner, "Magnetization-induced second harmonic generation from the Ni/Cu interface in multilayers on Cu(100)," Phys. Rev. B **63**, 0544-01 (2001).
10. V. N. Gridnev, "New approach to the theory of second harmonic generation in reflection and transmission of light," Solid State Commun. **100**, 71–75 (1996).
11. N. Hashizume, M. Ohashi, T. Kondo, and R. Ito, "Optical harmonic generation in multilayered structures: a comprehensive analysis," J. Opt. Soc. Am. B **12**, 1894–1904 (1995).